Quaternary Geochronology 18 (2013) 149–157

Contents lists available at SciVerse ScienceDirect

Quaternary Geochronology

journal homepage: www.elsevier.com/locate/quageo

Research paper

Cosmogenic-nuclide burial ages for Pleistocene sedimentary fill in Unaweep Canyon, Colorado, USA

Greg Balco [a,*], Gerilyn S. Soreghan [b], Dustin E. Sweet [c], Kristen R. Marra [b], Paul R. Bierman [d]

[a] Berkeley Geochronology Center, 2455 Ridge Road, Berkeley, CA 94709, USA
[b] School of Geology and Geophysics, University of Oklahoma, 100 E Boyd St., Norman, OK 73019, USA
[c] Department of Geosciences, Texas Tech University, Lubbock, TX 79409, USA
[d] Geology Department, University of Vermont, 180 Colchester Ave., Burlington, VT 05405, USA

ARTICLE INFO

Article history:
Received 28 September 2012
Received in revised form
15 February 2013
Accepted 21 February 2013
Available online 14 March 2013

Keywords:
Unaweep Canyon
Pleistocene
Cenozoic
River incision
River capture
Gunnison River
Colorado Plateau
Aluminum-26
Beryllium-10
Burial dating
Burial isochron dating

ABSTRACT

We applied both single-sample and isochron methods of cosmogenic-nuclide burial dating to determine the age of the sedimentary fill in Unaweep Canyon, western Colorado, USA. This stratigraphic sequence is of interest because it documents capture and diversion of the ancestral Gunnison River by the Colorado River during late Cenozoic incision of the Colorado Plateau. Seven ^{26}Al–^{10}Be burial ages from sedimentary infill penetrated by a borehole in central Unaweep Canyon, as well as a ^{26}Al–^{10}Be burial isochron age formed by multiple clasts and grain-size separates in a sample from the stratigraphically lower Gateway gravels, indicate that canyon blockage, initiation of lacustrine sediment accumulation, and presumed river capture, took place 1.41 ± 0.19 Ma. Lacustrine sedimentation ceased 1.34 ± 0.13 Ma.

1. Unaweep Canyon

Unaweep Canyon forms a 70-km-long wind gap through the Uncompaghre Plateau in western Colorado, exposing Proterozoic basement beneath the Mesozoic cover of the plateau. It stretches from near the confluence of the Colorado and Gunnison Rivers near its northeast end to the Dolores River near its southwest end (Fig. 1). The name "Unaweep" ("canyon with two mouths") denotes the fact that it currently contains two small streams (East Creek and West Creek) flowing away from a topographic divide at 2150 m elevation in the center of the canyon (Figs. 1 and 2). Beginning with the Hayden Survey of the late 1800's (Peale, 1877; Gannett, 1882), all observers have agreed that the drainage area of modern East and West Creeks is inadequate to account for canyon incision. Although the canyon has been hypothesized to have been formed by Quaternary glacial erosion (Cole and Young, 1983), its low elevation relative to other glaciated parts of the Rockies makes this unlikely. Most researchers agree that the canyon was formed by late Cenozoic fluvial incision due to past occupation by the Gunnison River, the Colorado River, or both (Peale, 1877; Gannett, 1882; Cater, 1966; Hunt, 1969; Sinnock, 1978; Lohman, 1981; Steven, 2002; Aslan et al., 2005; Soreghan et al., 2007, 2008). Soreghan et al. (2007, 2008) further argued that the canyon was originally formed in Proterozoic basement by Permo-Pennsylvanian glacial erosion, buried by late Paleozoic sedimentary fill, and re-exposed by Cenozoic incision. However, this hypothesis is not relevant to the Cenozoic incision history discussed in this paper.

Most previous work proposed that the canyon was abandoned by the Gunnison and/or Colorado Rivers due to tectonic arching of the Uncompaghre Plateau (Lohman, 1961, 1981; Cater, 1966; Hunt, 1969; Sinnock, 1981; Scott et al., 2001; Steven, 2002). In this hypothesis, the present arched long profile of the canyon would represent a deformed bedrock river profile. However, a geophysical survey by Oesleby (1978) and, subsequently, a drillcore collected by

* Corresponding author. Tel.: +1 510 644 9200; fax: +1 510 644 9201.
E-mail address: balcs@bgc.org (G. Balco).

1871-1014/$ – see front matter © 2013 Elsevier B.V. All rights reserved.
http://dx.doi.org/10.1016/j.quageo.2013.02.002

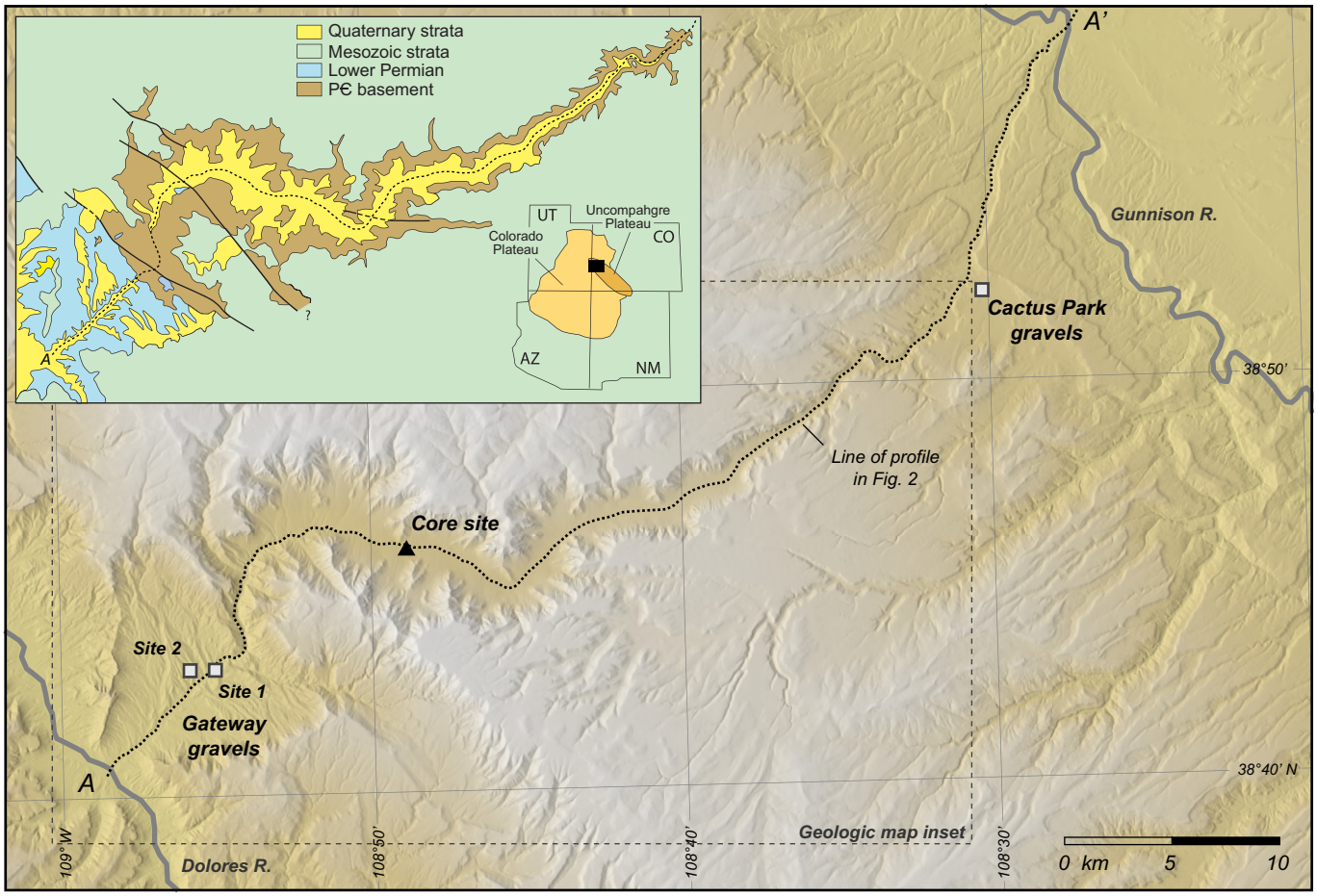

Fig. 1. Shaded-relief map of Unaweep Canyon. Inset shows simplified geologic map. The dotted line on both main map and inset is the line of the longitudinal section in Fig. 2.

Soreghan et al. (2007), showed that the canyon long profile does not reflect bedrock topography; rather, the canyon contains a thick fill of unconsolidated Cenozoic sediments (Fig. 2) overlying Paleozoic sedimentary rocks (Soreghan et al., 2007). The base of this sedimentary fill comprises sediment with Gunnison River provenance; additionally, gravels of similar lithology crop out at both ends of the canyon, recording past occupation of the canyon by an ancestral Gunnison River (Lohman, 1961, 1965; Aslan et al., 2005, 2008b; Kaplan, 2006). A thick (150 m) lacustrine succession overlies the former river channel in the subsurface in the central canyon; this presumably records creation of accommodation space within the canyon by damming of its downstream end. Surficial mapping in the western end of the canyon indicates that the blockage was most likely a large bedrock landslide (Kaplan, 2006; Marra, 2008). The lacustrine interval is capped by a series of paleosols and then by a further 150 m of locally derived, poorly sorted gravels (Marra, 2008). This upper unit is contiguous with modern alluvial fan deposition from canyon walls. Thus, the subsurface

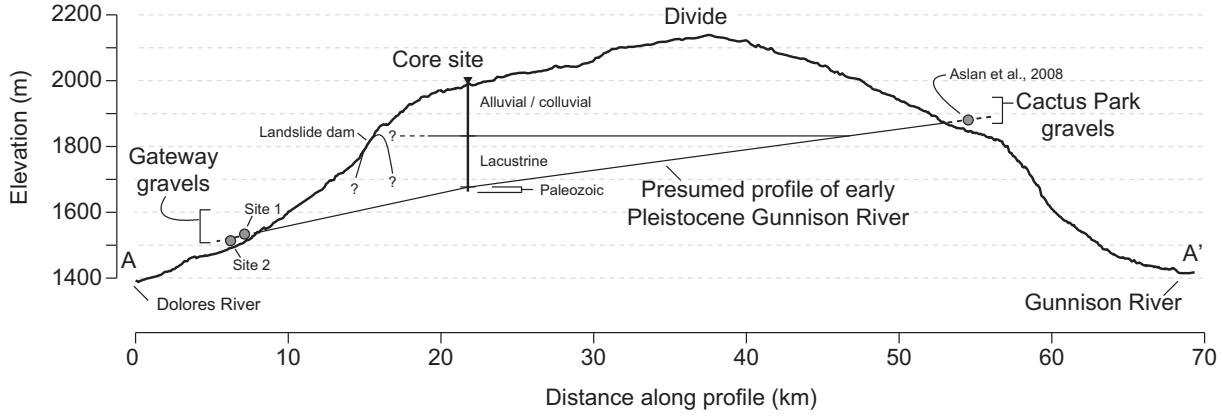

Fig. 2. Longitudinal section through Unaweep Canyon (see Fig. 1 for section line) showing stratigraphy of sedimentary fill. Brackets marked Gateway gravels and Cactus Park gravels show the elevation range of outcrops of these gravel units; filled circles show sites where burial-dating samples were actually collected (also see Fig. 1).

stratigraphic section in the central canyon records complete filling of the lake followed by additional subaerial accumulation of alluvial and/or colluvial sediment derived from hillslope erosion.

These stratigraphic relationships show that neotectonic uplift of the Uncompaghre Plateau is not required to explain canyon abandonment. Presumably, the landslide dam of the canyon caused capture and diversion of the Gunnison River into its present course. Thus, canyon abandonment was the result of river capture during regional Cenozoic incision.

In this paper, we use the technique of cosmogenic-nuclide burial dating to determine the age of the sedimentary fill in Unaweep Canyon. Previous estimates of the age of canyon abandonment were mostly based on comparison of the depth of incision by the present Gunnison River below the basal gravels in Unaweep Canyon (700 m) with regional incision rates inferred from a variety of evidence. These analyses suggested canyon abandonment sometime between 0.8 and 3.1 Ma (Kaplan, 2006; Aslan et al., 2008b). A single cosmogenic-nuclide measurement from the ancestral Gunnison River gravels exposed at Cactus Park at the east end of Unaweep Canyon (Figs. 1 and 2) yielded an apparent burial age of 1.06 ± 0.38 Ma (Aslan et al., 2008a), which presumably represents a basal age for the canyon fill. This paper describes additional cosmogenic-nuclide burial ages from 14 samples of both the basal gravels and the sedimentary fill penetrated by the borehole in the central canyon.

2. Stratigraphic context of samples

We collected samples from two sites: the borehole in the central canyon (Soreghan et al., 2007; Marra, 2008) and the basal Gunnison River gravels exposed at sites in the west end of the canyon. Here we describe the stratigraphic context of these samples as it pertains to the assumptions needed to compute cosmogenic-nuclide burial ages.

The borehole is located at 38°46.05 N, 108°48.86 W, at an elevation of 1994 m (Fig. 1). We collected two samples from the lacustrine unit that is the lowest Cenozoic unit in the borehole (202.4 and 243.6 m depth; Fig. 2; Table 1). This unit spans 120 m of core and generally coarsens upward from clay and silt to medium sand; the stratigraphic levels we sampled were relatively sandy. The composition of this unit indicates a Gunnison River provenance (Soreghan et al., 2007; Marra, 2008), so we assume that these sediments were derived from surface erosion in the watershed of the Gunnison River upstream of Cactus Park. Because they were deposited in a lake whose surface elevation was near 1825 m (Fig. 2), they experienced instantaneous burial in ~35 and ~80 m of water, respectively.

Two samples collected from the paleosol sequence capping the lacustrine unit (164.3 and 164.6 m depth) consisted of fine to medium sand with the same lithology as the underlying lacustrine sediments. Thus, they were also derived from erosion in the upstream Gunnison basin. However, they were deposited at or near the time of complete lake filling, so they were not instantaneously buried at the time of deposition. Instead, they were gradually buried as the overlying section accumulated.

We collected two samples (one at 112.7 m depth and one at 116.6 m depth) from the upper colluvial unit in the borehole. This unit consists of poorly sorted, crudely stratified sand and gravel containing clasts of Mesozoic sandstone and Precambrian basement that match lithologies exposed on nearby canyon walls. Thus, this unit was derived from erosion of the canyon walls near the borehole site. We sampled the sandy matrix of this unit. Again, these samples were not buried instantaneously but gradually as the overlying section accumulated.

Finally, we collected samples of the basal Gunnison River gravels from two sites at the western end of the canyon (Figs. 1–3). These sites expose the Gateway Gravels of Kaplan (2006), which consist of clast-supported fluvial cobble gravel containing volcanic rocks of Gunnison River provenance. The Gateway gravels occur atop bedrock straths between 1514 and 1615 m and represent at least three terrace levels. Our sample sites lie on the lowest of these. Paleocurrent indicators indicate flow to the west, consistent with canyon occupation by a paleo-Gunnison River (Kaplan, 2006). They are presumably correlative with the Cactus Park gravels at the eastern end of the canyon (Fig. 2). We collected samples at two sites (Fig. 3). At one site where these gravels were exposed in a newly excavated gravel pit ("Site 2" in Table 1 and Figs. 1 and 2; 38°43.16 N, 108°65.07 W, 1515 m elevation), we collected three cobble-sized clasts of quartz-rich lithologies (quartzite and felsic intrusive) as well as samples of the sandy matrix. At a second, natural, exposure ("Site 1"; 38°43.16 N, 108°55.88 W, 1534 m elevation), we excavated ~1 m beneath the present surface and collected a single sample of 55 clasts of pebble gravel. We presume that all these samples originated from surface erosion in the upstream Gunnison watershed. However, these gravels are at present only 1–5 m thick at our sample sites, and it is unclear what their original depositional thickness was. Thus, we have little constraint on the postdepositional burial depths of these samples. As discussed in more detail later, we address this issue by applying an isochron method of burial dating that does not require knowledge of this information.

3. Analytical methods and results

We extracted quartz from these samples by crushing (the clasts), sieving to appropriate grain sizes (crushed clasts and sediment samples) and repeated etching in dilute HF. Al and Be extraction and purification took place at two laboratories, at the U. of Washington and the U. of Vermont, and involved standard methods of HF dissolution and column chromatography (Stone, 2004). Both labs employed a ^{9}Be carrier prepared from deep-mined beryl. We measured total Al concentrations by ICP-OES at UW and UVM, and measured Al and Be isotope ratios by accelerator mass spectrometry at the Center for Accelerator Mass Spectrometry, Lawrence Livermore National Laboratory. Total carrier and process blanks at UW and UVM contained 18,000 ± 4000 and 9000 ± 2000 atoms ^{10}Be respectively (0.1–1.5% of total ^{10}Be present) and 65,000 ± 40,000 and 375,000 ± 215,000 atoms ^{26}Al respectively (0.01–0.2% of total ^{26}Al present). Table 1 and Figs. 4 and 5 show ^{10}Be and ^{26}Al concentrations. Both UW and UVM analyzed replicate splits of purified quartz for one sample (UNW04-369.5, at 112.7 m depth in the borehole); results agree at stated uncertainties (Table 1).

4. Burial age computations

The method of calculating a burial age from measured cosmogenic nuclide concentrations depends on the exposure and burial history of the sample. Thus, interpreting ^{10}Be–^{26}Al measurements as a burial age involves i) using geologic evidence to determine the sequence of exposure and burial events that the sample experienced, and then ii) choosing a calculation method appropriate to that exposure-burial history.

The simplest approach to burial dating applies when the following conditions are met: i) a sample originates from a surface that has been experiencing steady erosion for long enough that cosmogenic-nuclide concentrations have reached equilibrium with the erosion rate; ii) the sample is rapidly transported to its present location and buried to its present depth; and iii) the sample has

Table 1
Cosmogenic-nuclide concentrations and burial ages. Burial ages shown in bold are those that are consistent with geomorphic and stratigraphic constraints; other ages are calculated using assumptions that are inconsistent with these constraints and are included here as examples to support discussion in the text. Sample names in *italics* were processed at the University of Vermont; others were processed at the University of Washington. Uncertainties not in parentheses are "internal" uncertainties reflecting measurement uncertainty only; those in parentheses are "external" uncertainties reflecting both measurement and decay constant uncertainty.

Sample name	Depth in core (m)	Grain size (mm)	$[^{10}Be]$[a] (10^3 atoms g^{-1})	$[^{26}Al]$[b] (10^3 atoms g^{-1})	Instantaneous burial[c]		Steady accumulation[d]		Burial isochron age (Ma)
					Burial age (Ma)	Apparent erosion rate (m Myr^{-1})	Burial age (Ma)	Apparent erosion rate (m Myr^{-1})	
Core samples from Unaweep Canyon borehole									
UNW04-369.5-1	112.7	0.25–0.85	111.9 ± 3.8	496 ± 142	0.87 ± 0.61 (0.61)	87 ± 26 (28)	**0.95 ± 0.65 (0.66)**	**310 ± 210 (220)**	–
UNW04-369.5-2	112.7	0.25–0.85	114.4 ± 2.2	462 ± 38	1.07 ± 0.18 (0.19)	77.1 ± 7.3 (10.9)	**1.16 ± 0.19 (0.25)**	**342 ± 60 (117)**	–
UNW04-382.5	116.6	0.25–0.85	150.7 ± 5.9	720 ± 50	0.71 ± 0.16 (0.17)	69.7 ± 7.4 (10.3)	**0.76 ± 0.17 (0.19)**	**125 ± 10 (22)**	–
UNW04-539	164.3	0.125–0.5	321.7 ± 8.0	1125 ± 74	1.34 ± 0.14 (0.16)	26.3 ± 2.2 (3.6)	**1.37 ± 0.15 (0.17)**	**32.7 ± 2.6 (5.4)**	–
UNW04-540	164.6	0.125–0.5	296.1 ± 8.1	1085 ± 107	1.25 ± 0.21 (0.22)	30.1 ± 3.5 (4.7)	**1.27 ± 0.21 (0.23)**	**37.8 ± 4.0 (6.8)**	–
UNW04-664	202.4	0.25–0.85	248.4 ± 6.2	736 ± 155	**1.69 ± 0.44 (0.45)**	**28.7 ± 6.4 (7.2)**	–	–	–
UNW04-799	243.6	0.125–0.5	341.9 ± 8.7	1198 ± 103	**1.33 ± 0.18 (0.20)**	**25.8 ± 2.6 (3.7)**	–	–	–
Gunnison gravels, site 1									
09-GUNN-1-PEBBLES	–	10–40	373.0 ± 9.3	1287 ± 72	1.36 ± 0.12 (0.14)[e]	22.4 ± 1.7 (3.0)[e]	–	–	–
Gunnison gravels, site 2									
09-GUNN-2-CLAST-C	–	60	167.9 ± 4.2	582 ± 53	1.37 ± 0.20 (0.21)[e]	50.0 ± 5.4 (7.5)[e]	–	–	**1.46 ± 0.33 (0.34)**
09-GUNN-2-CLAST-D	–	55	110.3 ± 2.8	330 ± 56	1.67 ± 0.36 (0.37)[e]	65 ± 12 (14)[e]	–	–	
09-GUNN-2-CLAST-E	–	70	88.9 ± 2.3	351 ± 34	1.11 ± 0.21 (0.21)[e]	108 ± 12 (17)[e]	–	–	
09-GUNN-2-MTX-C	–	0.71–1	60.7 ± 1.9	237 ± 44	1.13 ± 0.39 (0.39)[e]	155 ± 31 (35)[e]	–	–	
09-GUNN-2-MTX-M	–	0.5–0.71	62.3 ± 2.0	189 ± 48	1.65 ± 0.53 (0.54)[e]	118 ± 32 (34)[e]	–	–	
09-GUNN-2-MTX-F	–	0.25–0.5	79.7 ± 2.3	252 ± 42	1.56 ± 0.35 (0.36)[e]	96 ± 17 (20)[e]	–	–	

[a] Normalized to the "07KNSTD" Be isotope ratio standard series. See Nishiizumi et al. (2007).
[b] Normalized to the "KNSTD" Al isotope ratio standard series. See Nishiizumi (2004).
[c] Calculated assuming initial equilibrium with steady erosion followed by a single period of burial at the present depth of the samples (Equations (1) and (2) in text).
[d] Calculated assuming initial equilibrium with steady erosion, followed by slow burial by steady sediment accumulation between the time of sample emplacement and the present (Equations (3) and (4) in text).
[e] Assumes both instantaneous and infinite burial.

Fig. 3. Photographs of sample sites in Gateway Gravels. Upper photo, site 1; lower photo, site 2. At both sites, cobble gravels of Gunnison River provenance overlie straths incised into Cutler formation sandstones and siltstones.

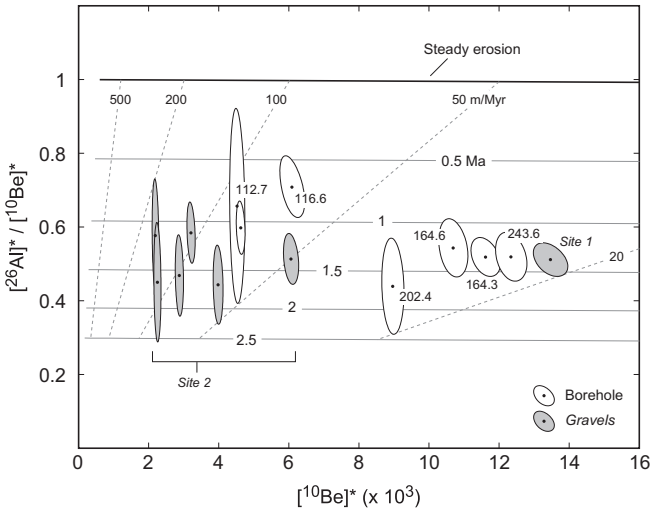

Fig. 4. Normalized ^{26}Al and ^{10}Be concentrations plotted on an exposure-burial diagram (Granger (2006) describes in detail the construction and use of this diagram). Nuclide concentrations in samples from the Gateway gravels and below 164 m in the borehole are normalized to mean production rates for the modern Gunnison River watershed upstream of Cactus Park (see text for details). Nuclide concentrations in samples from the colluvial section above 164 m depth in the borehole are normalized to production rates appropriate to the mean elevation of the canyon wall adjacent to the drill site. The numbers adjacent to the ellipses corresponding to borehole samples indicate depths in the borehole (see Table 1). Following common practice for this diagram, isolines of burial age and pre-burial erosion rate are computed on the basis of instantaneous burial at infinite depth. As described in the text, these assumptions are not consistent with the geological context of the samples. Thus, burial age estimates that correctly account for geological constraints, as described in the text and shown in Table 1, differ from the apparent burial ages inferred from this diagram. The ellipses are 68% confidence regions.

remained buried at that depth until the time of collection. In this case, ^{10}Be and ^{26}Al concentrations are:

$$N_{10} = \frac{P_{10,w}}{\lambda_{10} + \varepsilon/\Lambda_{sp}} e^{-\lambda_{10} t_b} + \frac{P_{10,s}}{\lambda_{10}} \left(1 - e^{-\lambda_{10} t_b}\right) \quad (1)$$

$$N_{26} = \frac{P_{26,w}}{\lambda_{26} + \varepsilon/\Lambda_{sp}} e^{-\lambda_{26} t_b} + \frac{P_{26,s}}{\lambda_{26}} \left(1 - e^{-\lambda_{26} t_b}\right) \quad (2)$$

where: N_{10} and N_{26} are ^{10}Be and ^{26}Al concentrations at the present time (atoms g^{-1}); $P_{10,w}$ and $P_{26,w}$ are mean surface production rates of ^{10}Be and ^{26}Al in the watershed from which the sediment is derived (atoms g^{-1} yr^{-1}); $P_{10,s}$ and $P_{26,s}$ are production rates of ^{10}Be and ^{26}Al at the present location and burial depth of the sample (atoms g^{-1} yr^{-1}); λ_{10} is the ^{10}Be decay constant (4.99×10^{-7} yr^{-1}); λ_{26} is the ^{26}Al decay constant (9.83×10^{-7} yr^{-1}); ε is the mean erosion rate, at the time of sample burial, in the watershed from which the sediment is derived (g cm^2 yr^{-1}); Λ_{sp} is an effective attenuation length for spallogenic production (g cm^2); and t_b is the burial duration (yr). Granger (2006) describes these equations in additional detail. These equations (as well as Equations (3) and (4) below) disregard production due to muons during initial exposure of the samples during erosion of the watershed (the first terms in Equations (1) and (2)); this introduces a small inaccuracy in the inferred erosion rate prior to burial (see additional discussion in Balco et al., 2008), but as we are interested primarily in the burial age in this work, we accept this tradeoff of accuracy for simplicity. However, in nearly all burial-dating situations, the post-burial nuclide production (the second terms in Equations (1) and (2)) is mainly due to muon interactions; we describe how we compute production rates due to muons below.

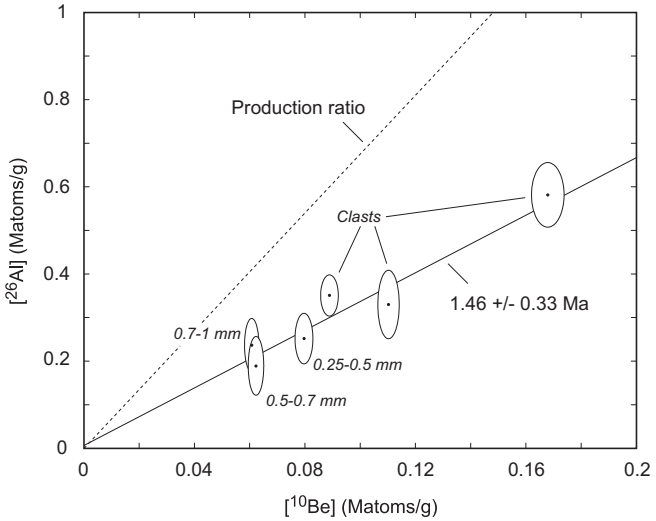

Fig. 5. ^{26}Al–^{10}Be burial isochron diagram (Balco and Rovey, 2008) for samples from Gateway Gravels at site 2 (Fig. 1; Table 1). Ellipses are 68% confidence regions.

Equations (1) and (2) contain two unknown parameters: the source area erosion rate ε and the burial age t_b. As we have two measurements (^{10}Be and ^{26}Al concentrations), the pair of equations can be solved for both unknowns. These equations apply to our two deepest borehole samples (202 and 244 m depth); geologic evidence indicates that these sediments were derived from surface erosion in the upstream Gunnison catchment and buried instantaneously by deposition in a lake. Strictly, they did not remain at a constant depth between the time of burial and the present, because after lake filling they were further buried by accumulation of the upper alluvial fan unit. However, the initial burial was deep enough ($\sim$35 and $\sim$80 m for the two samples) to make subsequent nuclide accumulation negligible, so assuming a single period of burial at constant depth does not have a significant effect on the inferred burial age. Thus, we calculated burial ages for these samples using Equations (1) and (2) with present burial depths and values of $P_{10,w}$ and $P_{26,w}$ appropriate for the Gunnison watershed upstream of Cactus Park (following Balco et al. (2008) and Stone (2000), 28 and 189 atoms g^{-1} yr^{-1} respectively).

Geological evidence indicates that the other four samples in the borehole were also derived from surface erosion (in the upstream Gunnison catchment for samples at 165–165 m depth and on the nearby canyon walls for samples at 112.7 and 116.6 m). However, they were not buried instantaneously, but rather gradually by accumulation of subaerially deposited alluvial sediment. Given steady accumulation between the time of sample emplacement and the present, ^{10}Be and ^{26}Al concentrations are:

$$N_{10} = \frac{P_{10,w}}{\lambda_{10} + \varepsilon/\Lambda_{sp}} e^{-\lambda_{10} t_b} + \frac{P_{10,s}}{\frac{Z}{t_b \Lambda_{sp}} - \lambda_{10}} e^{\frac{-Z}{\Lambda_{sp}}} \left[e^{t_b \left(\frac{Z}{t_b \Lambda_{sp}} - \lambda_{10} \right)} - 1 \right] + \int_0^{t_b} P_{10,\mu}(Z - Z\tau/t_b) e^{-\tau \lambda_{10}} \mathrm{d}\tau \quad (3)$$

$$N_{26} = \frac{P_{26,w}}{\lambda_{26} + \varepsilon/\Lambda_{sp}} e^{-\lambda_{26} t_b} + \frac{P_{26,s}}{\frac{Z}{t_b \Lambda_{sp}} - \lambda_{26}} e^{\frac{-Z}{\Lambda_{sp}}} \left[e^{t_b \left(\frac{Z}{t_b \Lambda_{sp}} - \lambda_{26} \right)} - 1 \right] + \int_0^{t_b} P_{26,\mu}(Z - Z\tau/t_b) e^{-\tau \lambda_{26}} \mathrm{d}\tau \quad (4)$$

where Z is the current burial depth of the sample (g cm^{-2}) and $P_{10,\mu}(z)$ and $P_{26,\mu}(z)$ are production rates (atoms g^{-1} yr^{-1}) for ^{10}Be and ^{26}Al due to muon interactions as a function of depth z (g cm^{-2}). τ is a variable of integration. Thus, we calculated burial ages for the upper four borehole samples using Equations (3) and (4) (Table 1). For samples at the top of the lacustrine sequence (at 164.3 and 164.6 m) we used source production rates $P_{10,w}$ and $P_{26,w}$ appropriate to the upstream Gunnison watershed as discussed above; for samples in the overlying alluvial section we used source production rates appropriate to the mean elevation of the nearby canyon wall (following Balco et al. (2008) and Stone (2000), 25 and 167 atoms g^{-1} yr^{-1} respectively). Table 1 also shows burial ages for these samples calculated using Equations (1) and (2); although these results are inconsistent with the geological evidence, the comparison shows that burial ages inferred from Equations (1–2) and (3–4) are similar (Equations (3) and (4) yield slightly older ages), but implied pre-burial erosion rates can be very different. This is important because it highlights the fact that, as long as the accumulation rate is relatively fast (order 10 cm kyr^{-1}) the burial age is relatively insensitive to the assumption of steady accumulation. However, the inferred pre-burial erosion rate can be very sensitive to this assumption. Balco and Stone (2005) discuss this issue in detail.

Note that both Equations (1–2) and (3–4) require computing subsurface production rates. At depths below a few meters, production is due to muon interactions. We computed production rates due to muons by calculating subsurface muon fluxes and stopping rates using the MATLAB implementation in Balco et al. (2008) of the method of Heisinger et al. (2002b, a). Instead of the muon interaction cross-sections determined experimentally by Heisinger, however, we used cross-sections inferred from ^{10}Be and ^{26}Al concentrations in a deep sandstone borehole in Beacon Valley, Antarctica, collected as part of the CRONUS-Earth project (John Stone, written communication, 2012). These cross-sections are: for ^{10}Be, $f^* = 0.0011$ and $\sigma_0 = 0.81$ μb; for ^{26}Al, $f^* = 0.0084$ and $\sigma_0 = 13.6$ μb (these symbols correspond to those used by Heisinger et al.). These predict lower production rates than predicted by the Heisinger measurements (for example, at sea level and high latitude predicted muon production rates are reduced by 62% and 57% for ^{10}Be and ^{26}Al, respectively), and appear to resolve most differences between the Heisinger predictions and a variety of geological observations (e.g., Balco et al., 2008; Braucher et al., 2012, and references therein).

For samples collected from the Gateway gravels at the west end of the canyon, geological evidence shows that the samples were derived from surface erosion in the upstream Gunnison catchment. However, we cannot use either set of equations above to compute burial ages, because we have few geologic constraints on the burial depths of these samples after emplacement. Not only do we have limited information about the original depositional thickness of the gravels, we do not know when, or how fast, the sample sites were exposed by recent surface erosion. Balco and Rovey (2008) (p. 1104–1105) described a method of dealing with this situation by collecting a set of individual clasts from fluvial sediment. These clasts are likely to be derived from different regions of the watershed subject to different surface erosion rates and/or nuclide production rates, but they are buried together so that they all share the same postdepositional nuclide production. Without knowledge of the actual amount of postdepositional nuclide production, a burial age for any individual clast, or single sample of agglomerated clasts, computed using Equations (1) and (2) is not accurate (except possibly by accident). However, if all clasts share the same postdepositional burial history, the ^{10}Be and ^{26}Al concentrations from all clasts will form a linear array, that is, an isochron, in ^{10}Be–^{26}Al space. Regardless of the amount of postdepositional nuclide accumulation, the slope of this isochron depends only on the burial age of the sample. Balco and Rovey (2008) also described an iterative scheme to account for situations where the initial ^{26}Al/^{10}Be ratio in samples derived from slowly eroding landscapes differs from the production ratio, but this is not necessary in the present case because nuclide concentrations in these samples are relatively low, implying erosion rates high enough ($>\sim$80 m Myr^{-1}; see Fig. 4) that the divergence of the initial ratio from the production ratio is negligible ($<\sim$1%) when compared with measurement uncertainty.

We applied this method to the set of samples we collected from the Gateway gravels at our site 2. In addition to individual clasts, we also analyzed a range of grain-size fractions from the sandy matrix at this site (Table 1). Like individual clasts, different sediment grain sizes commonly originate from different sources in the watershed and have different nuclide concentrations (e.g., Balco and Stone, 2005; Brown et al., 1995). As expected from this reasoning, measured ^{10}Be and ^{26}Al concentrations from both clasts and sand

grain-size fractions at this site form an isochron in ^{10}Be–^{26}Al space, whose slope is less than the $^{26}Al/^{10}Be$ production ratio and whose *y*-intercept is greater than zero (Fig. 5). The isochron slope (computed using the regression scheme of York (1966); see Balco and Rovey (2008)) implies an age of 1.46 ± 0.33 Ma for the Gateway gravels at site 2. The *y*-intercept is close to zero, indicating that postdepositional nuclide production at this site was relatively small. Thus, in this case, individual burial ages computed from each sample on the assumption of instantaneous, infinite burial (using Equations (1) and (2); see Table 1 and Fig. 4) closely approximate the isochron age. However, there is no way to know this in advance from geological information.

The same geological constraints apply at our other sample site in the Gateway gravels (site 1; Table 1; Figs. 1 and 2). However, at this site we only analyzed a single sample of agglomerated pebbles, so we cannot compute an isochron age. Assuming instantaneous, infinite burial yields a burial age of 1.36 ± 0.12 Ma. If the burial history at this site was similar to that at site 2, this is most likely a close approximation of the true emplacement age, and, in fact, it agrees with the isochron age at site 2. However, lacking geological constraints on the burial history, strictly this is a minimum age for the gravels at this site.

5. Discussion

Our best estimate of the age of the Gateway gravels is the isochron age of 1.46 ± 0.33 Ma from sample site 2; this age must be equal to or older than the age of canyon abandonment. Burial ages on the lacustrine unit in the borehole of 1.33 ± 0.18 and 1.69 ± 0.44 must be younger than the age of canyon abandonment. These ages all agree within their respective uncertainties and imply canyon abandonment near 1.4 Ma. The rest of the burial ages from higher up in the borehole are consistent, within uncertainties, with their stratigraphic order (Fig. 6).

To derive a summary age model and uncertainty estimate for the data set as a whole, we assumed the following: i) our isochron age for the lowest Gateway gravels represents the time of canyon abandonment; ii) the lower lacustrine unit in the borehole accumulated at a constant accumulation rate; and iii) the upper colluvial unit in the borehole accumulated at a constant rate between the time of lake filling and the present. This implies a two-stage, piecewise-linear, age model with two free parameters: i) the age of canyon abandonment and beginning of lacustrine sediment accumulation; and ii) the age of lake filling and transition from lacustrine to subaerial sediment accumulation (Fig. 6). An error-weighted least squares fit of this age model to the Gateway gravels isochron age and all seven burial ages from the borehole (Fig. 6) yields best-fitting ages for canyon abandonment and lake infilling of 1.41 and 1.34 Ma, respectively. This age model fits this data set with a reduced chi-squared statistic of 0.6, indicating that the scatter of the data is consistent with measurement uncertainties, and also that a more complex age model is not required or justified by the observations. We estimated the uncertainty in this age model by a Monte Carlo simulation in which we repeatedly sampled sets of burial ages given the assumptions that ages were subject to normally distributed measurement errors ("internal uncertainties" in Table 1), and fit the two-parameter age model to each sample. This procedure yielded distributions of canyon abandonment and lake filling ages having standard deviations of 0.17 and 0.10 Myr, respectively. Propagating additional decay

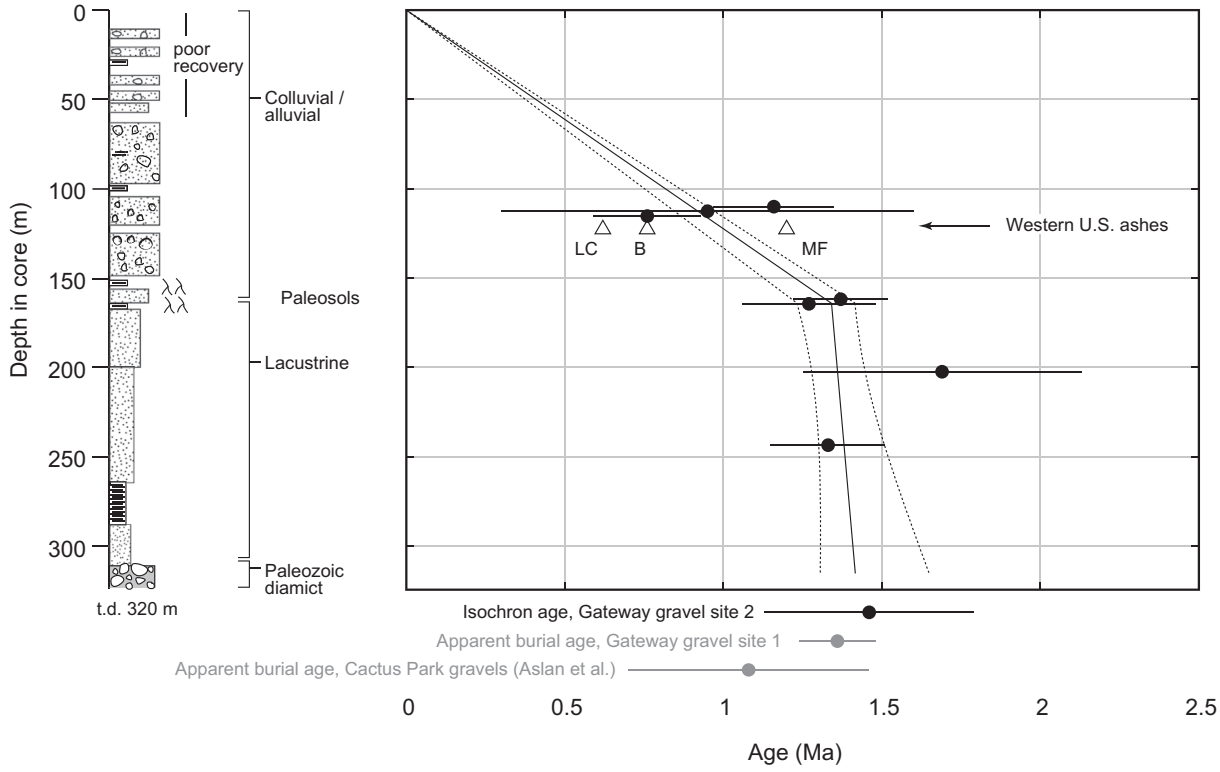

Fig. 6. Stratigraphic section (adapted from Soreghan et al. (2007)) and summary age model for Unaweep Canyon sedimentary fill. The solid line shows a two-parameter, piecewise-linear age model fit to the isochron burial age for the Gateway gravels at our site 2 and the burial ages from borehole samples (burial ages used to fit the age model are shown by black symbols here and in bold in Table 1; see text for details). Error bars show 1σ measurement uncertainties. Dashed lines show a 68% confidence estimate based on a Monte Carlo simulation (see text). Apparent burial ages based on single samples from the Gateway gravels at our site 1 (see Table 1) and the Cactus Park gravels (Aslan et al., 2008a) are shown in gray. Open triangles show ages of widely distributed western U.S. ashes, plotted at the depth of an unidentified ash in the borehole (see text).

constant uncertainties into this result increases these to 0.19 and 0.13 Ma, respectively.

To summarize, we conclude that the canyon-blocking landslide, that initiated lacustrine sedimentation and presumably also caused diversion of the paleo-Gunnison River into its present course, took place 1.41 ± 0.19 Ma. Complete filling of the lake and commencement of subaerial sediment accumulation at the borehole site took place 1.34 ± 0.13 Ma. As discussed above, in calculating this we assumed that the youngest Gateway gravels were active at the time of canyon blockage. To evaluate the importance of this, we relaxed this assumption and fit the age model only to burial ages from the borehole without considering the isochron age. This yielded a basal age for the borehole of 1.37 ± 0.22 Ma (measurement uncertainties only), which is indistinguishable from the isochron age for the Gateway gravels. Thus, our observations are consistent with the hypothesis that the youngest Gateway gravels represent the active river channel immediately before canyon abandonment.

There are several independent constraints on the age of canyon abandonment and the sedimentary section in the borehole that we can use to evaluate these conclusions. First, Aslan et al. (2008a) obtained a single burial age of 1.06 ± 0.38 from the lowest Cactus Park gravels at the east end of Unaweep Canyon (Figs. 1 and 2). Although Aslan et al. (2008a) did not describe their calculations in detail, they interpreted it as an age for abandonment of Unaweep Canyon by the Gunnison River. This age estimate and our age estimate for the same event agree within uncertainties, which is consistent with the hypothesis that the Gateway and Cactus Park gravels are correlative and represent the course of the Gunnison River prior to canyon abandonment.

Second, the burial ages from the borehole imply a rate of lake infilling that we can compare with the expected sediment delivery from the upstream Gunnison basin. If we approximate the lacustrine sediment section in Unaweep Canyon as an (inverted) irregular pyramid with length ~35 km (Fig. 2), width ~3 km (Fig. 1), and thickness 230 m (Fig. 2), this implies a sediment volume of ~4 km^3. The area of the Gunnison watershed upstream of Cactus Park is 9500 km^2, so given rock and sediment densities of 2.7 and 2.2 g cm^{-3}, respectively, and complete trapping of sediment, the lacustrine sediment infill in the canyon would represent ~0.4 m erosion of the watershed. Basin-scale erosion rates inferred from nuclide concentrations in the lacustrine sediment section (Table 1) are 26–29 m Myr^{-1}, at which rate erosion of 0.4 m would require 15,000 yr. Thus, the expected sediment production from the Gunnison watershed is approximately an order of magnitude greater than required to fill the lake basin in the approximately 0.1 Myr implied by our best-fitting age model, and therefore does not contradict the age model. The duration of lake sediment accumulation inferred from the age model is substantially less than the uncertainties in the age model, so we can only conclude that this duration was less than ca. ~0.1–0.2 Myr. It is possible that the lake filled in substantially less than 100,000 years.

Third, Marra (2008) observed a weathered ash layer at 115 m depth in the borehole. Although the ash was too devitrified by postdepositional chemical alteration to permit either direct dating or geochemical fingerprinting (E. Wan, personal communication, 2008), it is most likely that this ash is one of the Lava Creek (0.62 Ma) or Mesa Falls (1.2 Ma) ashes from the Yellowstone volcanic center, or the Bishop Ash (0.76 Ma) from Long Valley Caldera. The age model discussed above implies an age of 0.93 ± 0.1 Ma for this depth (Fig. 5); although this does not agree exactly with any of the possible ashes, it is closest to the age of the Bishop ash and the precision of the ages is not adequate to reject this possibility. As the Bishop ash occurs nearby (e.g., Colman et al., 1986), it appears most likely that this ash is the Bishop.

6. Conclusions

An age model fit to i) seven ^{26}Al–^{10}Be burial ages from sedimentary infill penetrated by a borehole in central Unaweep Canyon, and ii) an ^{26}Al–^{10}Be burial isochron age for the stratigraphically lower Gateway gravels, indicates that canyon blockage and initiation of lacustrine sediment accumulation took place 1.41 ± 0.19 Ma. Lacustrine sedimentation then ceased 1.34 ± 0.13 Ma. This age model is consistent with all individual ages given their measurement uncertainties, as well as all independent stratigraphic and chronological constraints that we are aware of.

Acknowledgments

This work was partially funded by a grant from the National Science Foundation (EAR-0934259). Any opinions, findings, and conclusions or recommendations expressed in this material are those of the author(s) and do not necessarily reflect the view of the National Science Foundation. We thank L. Keiser and A. Shock for help in sample preparation, and J. Larsen for property access. Dylan Rood (Lawrence Livermore National Laboratory) was instrumental in carrying out the ^{26}Al–^{10}Be measurements.

Editorial handling by: D.Bourlès

References

Aslan, A., Hood, W., Karlstrom, K., Kirby, E., Granger, D., Betton, C., Darling, A., Benage, M., Schoepfer, S., 2008a. Abandonment of Unaweep Canyon Approximately 1 Ma and the Effects of Transient Knickpoint Migration, Western Colorado. Abstracts with programs. Geological Society of America, 2008 Annual Meeting 40, 220.

Aslan, A., Karlstrom, K., Hood, W., Cole, R., Oesleby, T., Betton, C., Sandoval, M., Darling, A., Kelley, S., Hudson, A., Kaproth, B., 2008b. River incision histories of the Black Canyon of the Gunnison and Unaweep Canyon: interplay between late Cenozoic tectonism, climate change, and drainage integration in the western Rocky Mountains. In: Raynolds, R. (Ed.), Roaming the Rocky Mountains and Environe: Geological Field Trips. Geological Society of America Field Guide, vol. 10, pp. 175–202.

Aslan, A., Livacarri, R., Hood, W., Betton, C., Garhart, A., 2005. Geological history of the Uncompaghre plateau and Unaweep Canyon. In: Guide to Field Trips, 2005 Annual Meeting, Geological Society of America Rocky Mountain Section. Grand Junction Geological Society.

Balco, G., Rovey, C., 2008. An isochron method for cosmogenic-nuclide dating of buried soils. American Journal of Science 308, 1083–1114.

Balco, G., Stone, J., Lifton, N., Dunai, T., 2008. A complete and easily accessible means of calculating surface exposure ages or erosion rates from ^{10}Be and ^{26}Al measurements. Quaternary Geochronology 3, 174–195.

Balco, G., Stone, J.O.H., 2005. Measuring middle Pleistocene erosion rates with cosmic-ray-produced nuclides in alluvial sediment, Fisher Valley, southeast Utah. Earth Surface Processes and Landforms 30, 1051–1067.

Braucher, R., Bourlès, D., Merchel, S., Romani, J.V., Fernadez-Mosquera, D., Marti, K., Léanni, L., Chauvet, F., Arnold, M., Aumaître, G., Keddadouche, K., 2012. Determination of muon attenuation lengths in depth profiles from in situ produced cosmogenic nuclides. Nuclear Instruments and Methods in Physics Research Section B: Beam Interactions with Materials and Atoms 294, 484–490.

Brown, E., Stallard, R., Larsen, M., Raisbeck, G.M., Yiou, F., 1995. Denudation rates determined from the accumulation of in-situ-produced ^{10}Be in the luquillo experimental forest, Puerto Rico. Earth and Planetary Science Letters 129, 193–202.

Cater, F.W.J., 1966. Age of the Uncompaghre Uplift and Unaweep Canyon, West-central Colorado. U.S. Geological Survey. Professional Paper 550-C, pp. C86–C92.

Cole, R., Young, R., 1983. Evidence for glaciation in Unaweep Canyon, Mesa County, Colorado. In: Averett, W. (Ed.), Field Guide to the Northern Paradox Basin – Uncompaghre Uplift. Grand Junction Geological Society, pp. 73–80.

Colman, S., Choquette, A., Rosholt, J., G.H. M, Huntley, D., 1986. Dating the upper Cenozoic sediments in fisher valley, southeastern Utah. Geological Society of America Bulletin 97, 1422–1431.

Gannett, H., 1882. The Unaweep Cañon (Colorado). Popular Science Monthly 20, 781–786.

Granger, D., 2006. A review of burial dating methods using ^{26}Al and ^{10}Be. In: Siame, L., Bourlès, D., Brown, E. (Eds.), 2006. In-situ-produced Cosmogenic Nuclides and Quantification of Geological Processes, vol. 415.

Geological Society of America, pp. 1–16. Geological Society of America Special Paper.
Heisinger, B., Lal, D., Jull, A.J.T., Kubik, P., Ivy-Ochs, S., Knie, K., Nolte, E., 2002a. Production of selected cosmogenic radionuclides by muons: 2. Capture of negative muons. Earth and Planetary Science Letters 200 (3–4), 357–369.
Heisinger, B., Lal, D., Jull, A.J.T., Kubik, P., Ivy-Ochs, S., Neumaier, S., Knie, K., Lazarev, V., Nolte, E., 2002b. Production of selected cosmogenic radionuclides by muons 1. Fast muons. Earth and Planetary Science Letters 200 (3–4), 345–355.
Hunt, C., 1969. The Colorado River Region and John Wesley Powell, Geologic History of the Colorado River. U.S. Geological Survey. Professional Paper 669-C, pp. C59–C130.
Kaplan, S., 2006. Revealing Unaweep Canyon: the Late Cenozoic Exhumation History of Unaweep Canyon as recorded by gravels in Gateway, Colorado. Master's thesis, University of Oklahoma.
Lohman, S., 1961. Abandonment of Unaweep Canyon, Mesa County, Colorado, by Capture of the Colorado and Gunnison Rivers. U.S. Geological Survey. Professional Paper 424, pp. B144–B146.
Lohman, S., 1965. Geology, Artesian Water Supply, Grand Junction Area, Colorado. U.S. Geological Survey. Professional Paper 451, pp. 69–74.
Lohman, S., 1981. Ancient drainage changes in and south of Unaweep Canyon, southwestern Colorado. In: Epis, R., Callender, J. (Eds.), Western Slope, Colorado: New Mexico Geological Society Guidebook, 32nd Field Conference. New Mexico Geological Society, pp. 137–143.
Marra, K., 2008. Late Cenozoic Geomorphic and Climatic Evolution of the Northeastern Colorado Plateau as Recorded by Plio-Pleistocene Sediment Fill in Unaweep Canyon, Colorado. Master's thesis, University of Oklahoma.
Nishiizumi, K., 2004. Preparation of Al-26AMS standards. Nuclear Instruments and Methods in Physics Research B 2004 (223–224), 388–392.
Nishiizumi, K., Imamura, M., Caffee, M., Southon, J., Finkel, R., McAnich, J., 2007. Absolute calibration of Be-10 AMS standards. Nuclear Instruments and Methods in Physics Research B 258, 403–413.
Oesleby, T., 1978. Uplift and Deformation of the Uncompaghre Plateau: Evidence from Fill Thickness in Unaweep Canyon, West-Central Colorado. Master's thesis, University of Colorado.
Peale, A., 1877. Geological Report on the Grand River District: U.S. Geological and Geographical survey of the Territories, Ninth Annual Report, pp. 31–102.
Scott, R., Harding, A., Hood, W., Cole, R., Livacarri, R., Johnson, J., Shroba, R., Dickerson, R., 2001. Geologic Map of Colorado National Monument and Adjacent Areas, Mesa County, Colorado. U.S. Geological Survey. Geologic Investigations Series I-2740.
Sinnock, S., 1978. Geomorphology of the Uncompaghre Plateau and Grand Valley, western Colorado. Master's thesis, Purdue University.
Sinnock, S., 1981. Pleistocene drainage changes in Uncompaghre Plateau-Grand Valley region of western Colorado, including formation and abandonment of Unaweep Canyon: a hypothesis. In: Western Slope, Colorado: New Mexico Geological Society Guidebook, 32nd Field Conference. New Mexico Geological Society, pp. 127–136.
Soreghan, G., Poulsen, C., Young, R., Eble, C., Sweet, D., Davogustto, O., 2008. Anomalous cold in the Pangaean tropics. Geology 36, 659–662.
Soreghan, G., Sweet, D., Marra, K., Eble, C., Soreghan, M., Elmore, R., Kaplan, S., Blum, M., 2007. An exhumed late Paleozoic canyon in the Rocky Mountains. Journal of Geology 115, 473–481.
Steven, T., 2002. Late Cenozoic tectonic and geomorphic framework surrounding the evaporite dissolution area in west-central Colorado. In: Late Cenozoic Evaporite Tectonism in West-central Colorado. Geological Society of America, pp. 15–30. Special Paper 366.
Stone, J., 2004. Extraction of Al and Be from Quartz for Isotopic Analysis. In: UW Cosmogenic Nuclide Lab Methods and Procedures. URL: http://depts.washington.edu/cosmolab/chem.html.
Stone, J.O., 2000. Air pressure and cosmogenic isotope production. Journal of Geophysical Research 105 (B10), 23753–23759.
York, D., 1966. Least-squares fitting of a straight line. Canadian Journal of Physics 44, 1079.